Technical Note: The effect of vertical turbulent mixing on gross O_2 production assessments by the triple isotopic composition of dissolved O_2

E. Wurgaft, O. Shamir, and A. Angert

The Freddy and Nadine Herrmann Institute of Earth Sciences, The Hebrew University of Jerusalem, Jerusalem, Israel

Correspondence to: E. Wurgaft (eyal.wurgaft@mail.huji.ac.il)

Abstract. The ^{17}O excess ($^{17}\Delta$) of dissolved O_2 has been used, for over a decade, to estimate gross O_2 production ($G^{17}OP$) rates in the mixed layer (ML) in many regions of the ocean. This estimate relies on a steady-state balance of O_2 fluxes, which include air–sea gas exchange, photosynthesis and respiration but notably, not turbulent mixing with O_2 from the thermocline. In light of recent publications, which showed that neglecting the turbulent flux of O_2 from the thermocline may lead to inaccurate $G^{17}OP$ estimations, we present a simple correction for the effect of this flux on ML $G^{17}OP$. The correction is based on a turbulent-flux term between the thermocline and the ML, and use the difference between the ML $^{17}\Delta$ and that of a single data-point below the ML base. Using a numerical model and measured data we compared turbulence-corrected $G^{17}OP$ rates to those calculated without it, and tested the sensitivity of the GOP correction for turbulent flux of O_2 from the thermocline to several parameters. The main source of uncertainty on the correction is the eddy-diffusivity coefficient, which induces an uncertainty of $\sim 50\%$. The corrected $G^{17}OP$ rates were 10–90 % lower than the previously published uncorrected rates, which implies that a large fraction of the photosynthetic O_2 in the ML is actually produced in the thermocline.

1 Introduction

Gross O_2 production (GOP) in the ocean is a fundamental process in the global cycling of O_2. As such, accurate estimates of GOP rates are essential in order to understand and model the global cycles of oxygen and carbon. During the past decade, the application of the triple isotope composition (^{16}O, ^{17}O, and ^{18}O) of dissolved O_2 as a tracer for GOP ($G^{17}OP$), which was first presented by Luz and Barkan (2000), has become widespread and has been used to estimate GOP rates in many regions of the ocean (Juranek and Quay, 2013, and refs. within).

1.1 GOP from $^{17}\Delta$

Estimating GOP rates from the isotopic composition of dissolved O_2 is based on the ^{17}O-excess ($^{17}\Delta$) that photosynthetically produced O_2 has in comparison to atmospheric O_2 (Luz et al., 1999). The $^{17}\Delta$ has been defined in several ways (Kaiser, 2011). A common definition (Miller, 2002; Luz and Barkan, 2005), which we use here is

$$^{17}\Delta = \ln(\delta^{17}O + 1) - \lambda \ln(\delta^{18}O + 1), \tag{1}$$

where $\delta^*O = (^*R_{\text{sample}}/^*R_{\text{ref}} - 1)$; $^*R_{\text{sample}}$ and $^*R_{\text{ref}}$ are the $^*O/^{16}O$ in the sample and the reference, respectively. λ is the slope of a reference line on a $\ln(\delta^{17}O+1)$ versus $\ln(\delta^{18}O+1)$ plot, which represents the expected slope of the relevant processes. Following Luz and Barkan (2005), most studies use $\lambda = 0.518$ for the calculation of $^{17}\Delta$ and atmospheric O_2 as a standard for the isotopic measurements. To derive a steady-state expression for GOP in the mixed layer (ML), Luz and Barkan (2000) used an O_2 and $^{17}\Delta$ 1-box model. Their derivation yielded the following equation:

$$G^{17}OP = K (O_2)_{\text{eq}} \frac{(^{17}\Delta_{\text{dis}} - ^{17}\Delta_{\text{eq}})}{(^{17}\Delta_{\text{p}} - ^{17}\Delta_{\text{dis}})}, \tag{2}$$

where K is the air–sea gas-exchange coefficient, $(O_2)_{\text{eq}}$ the equilibrium concentration of O_2 with the atmosphere, $^{17}\Delta_{\text{dis}}$

the $^{17}\Delta$ value of dissolved O_2, $^{17}\Delta_{eq}$ the equilibrium $^{17}\Delta$ with respect to atmospheric O_2, and $^{17}\Delta_p$ $^{17}\Delta$ at steady state between photosynthesis and respiration. Recently, Luz and Barkan (2000) method for ML GOP estimation (hereafter $G^{17}OP_{LB}$) was revised by Prokopenko et al. (2011) and Kaiser (2011), who derived equations for $G^{17}OP$ that use measured $\delta^{17}O$ and $\delta^{18}O$, the isotopic composition of dissolved O_2 in air–seawater equilibrium ($\delta^{17}O_{eq}$ and $\delta^{18}O_{eq}$), and the isotopic composition of photosynthetic O_2 ($\delta^{17}O_p$ and $\delta^{18}O_p$). Unlike Eq. (2), their equations avoided a number of numerical approximations. They did, however, rely on $\delta^{17}O_p$ and $\delta^{17}O_{eq}$ which are still subject to disagreement among researchers in the field (e.g. Kaiser and Abe, 2012). However, Luz and Barkan (2011a, b) and Nicholson (2011) showed that if proper $\delta^{17}O_p$ and $\delta^{18}O_p$ are assigned, the differences between $G^{17}OP_{LB}$ and the $G^{17}OP$ estimated by the revised versions are small.

1.2　The effect of turbulent mixing on $G^{17}OP$ estimation

As in Luz and Barkan (2000), the ML $G^{17}OP$ equations that were presented by Prokopenko et al. (2011) and Kaiser (2011) were derived with a 1-box representation of the ML in which a steady-state balance exists between the O_2 fluxes of GOP, respiration and air–sea gas exchange, but without accounting for the flux of turbulent mixing with O_2 from the thermocline. This was, in spite of the fact that vertical $^{17}\Delta$ profiles often show a pronounced increase below the ML base (Fig. 1; Luz and Barkan, 2000; Juranek and Quay, 2005; Quay et al., 2010). Juranek and Quay (2005) estimated that vertical turbulence had a negligible affect over $G^{17}OP$. However, Nicholson et al. (2012) showed that mixing of ML O_2 with high $^{17}\Delta$ O_2 from the thermocline into the ML (by either entrainment due to ML deepening, or by turbulent flux) may result in an overestimation of up to 80 % in ML $G^{17}OP$. Nicholson et al. (2012) further suggested that this overestimation was the likely explanation for the higher ratio of $G^{17}OP$ to ^{14}C-based net primary productivity ($G^{17}OP$: NPP(^{14}C); Marra, 2002; Juranek and Quay, 2005; Quay et al., 2010), compared to the ratio of GOP estimated from ^{18}O incubations to the same net productivity estimate ($G^{18}OP$: NPP(^{14}C)). In addition, Jonsson et al. (2013) found that the turbulent mixing had a considerable effect on estimation of net O_2 production, using O_2 : Ar measurements.

As noted above, high $^{17}\Delta$ O_2 from the thermocline can mix into the ML either by entrainment of water from the thermocline into the ML, which takes place as the ML base deepens, or by vertical turbulence of O_2 from the thermocline. The latter process dominates when the ML depth is constant (Fig. 1). Nicholson et al. (2012) did not consider these two process separately; however, their findings showed that $G^{17}OP$ overestimated GOP even when the ML depth was relatively constant, which indicates that vertical turbulence also affects $G^{17}OP$.
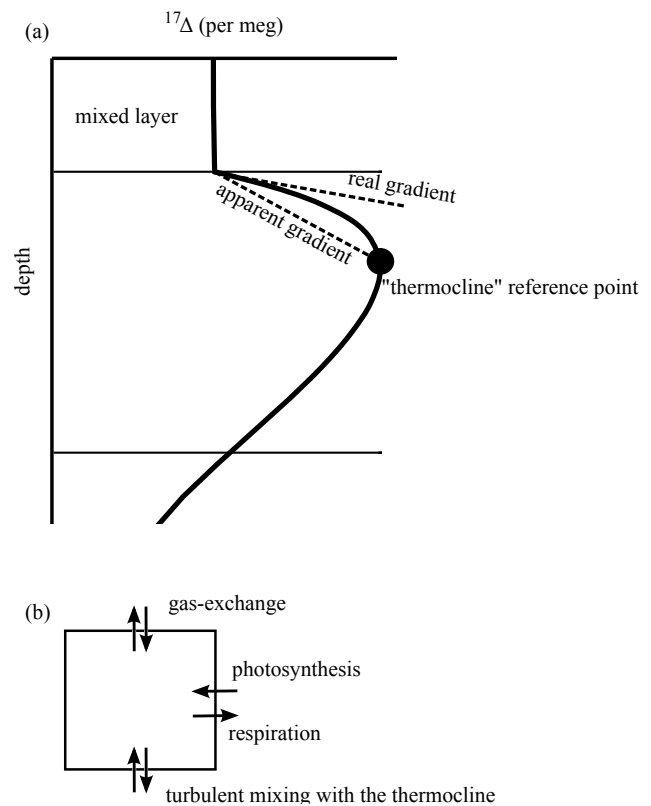
Fig. 1. (a) A schematic illustration of a typical mid-ocean $^{17}\Delta$ vertical profile. The dashed lines, which extend below the mixed-layer base define the $^{17}\Delta$ gradient, which in turn, is correlated with the $^{17}\Delta$ "flux" into the mixed layer. Depending on the profile shape, the choice of a "thermocline" reference point at some depth below the mixed-layer depth, results in a $^{17}\Delta$ gradient which is different than the real $^{17}\Delta$ gradient. **(b)** A conceptual model of the O_2 isotopologues fluxes in and out of the ML.

While Sarma et al. (2006) and Quay et al. (2010) discussed the effect of entrainment on $G^{17}OP$ and suggested non-steady-state corrections, and Castro-Morales et al. (2012) suggested a correction for the vertical flux of O_2 into the ML, the effect of turbulence on the triple isotopic composition and the resulting effect on ML $G^{17}OP$ estimations has not been explicitly examined. In light of Nicholson et al. (2012) and Jonsson et al. (2013) results, it is clear that to accurately estimate $G^{17}OP$ rates, the magnitude of the turbulent mixing effect should be evaluated, and if large, corrected for. The aims of this work were to evaluate the magnitude of the effect of turbulent mixing on ML $G^{17}OP$ estimation, and to derive an analytical correction for this effect.

2　Derivation of a GOP equation with a turbulent mixing term

Prokopenko et al. (2011) presented a new equation for $G^{17}OP$ ($G^{17}OP_{PRO}$), which was obtained by rigorous

derivation of time variations of O_2 isotopologues. We added a turbulent-flux term to Eq. (4) and Eq. (5) in Prokopenko et al. (2011). The turbulent flux was calculated between the base of the ML and a single point along the $^{17}\Delta$ gradient below the ML, which was assigned as "thermocline" (Fig. 1). Consequently, the $^{17}\Delta$ gradient below the ML was assumed to be linear with depth (we will revisit this assumption in sensitivity tests section). The resulting equation for the rate of change in $^{17}\Delta$ in the ML was (full derivation of the equation can be found in Appendix A):

$$
h\,(O_2)\frac{\partial(^{17}\Delta)}{\partial t} = G^{17}OP_C \left[\left(\frac{X_p^{17}-X^{17}}{X^{17}}\right) - \lambda\left(\frac{X_p^{18}-X^{18}}{X^{18}}\right)\right] \\
- K\,(O_2)_{eq}\left[\left(\frac{X^{17}-X_{eq}^{17}}{X^{17}}\right) - \lambda\left(\frac{X^{18}-X_{eq}^{18}}{X^{18}}\right)\right] \\
- \frac{\kappa}{Z}\,(O_2)_{thr}\left[\left(\frac{X^{17}-X_{thr}^{17}}{X^{17}}\right) - \lambda\left(\frac{X^{18}-X_{thr}^{18}}{X^{18}}\right)\right]
\tag{3}
$$

where h is the ML depth, (O_2) is the dissolved O_2 concentration in the ML, κ is the eddy-diffusivity coefficient, and Z is the vertical distance between the base of the ML and the depth assigned as "thermocline". For convenience, we use $D = \kappa/Z$ hereafter. X^* represents the ratio $^*O/^{16}O$. The subscripts "p" and "eq" denote "photosynthetic" and "equilibrium", respectively. Note that as was shown by Luz and Barkan (2009) and Prokopenko et al. (2011), the rate of change of $^{17}\Delta$ is independent of respiration. When steady-state conditions in the ML are assumed, the resulting term for turbulent-flux corrected $G^{17}OP$ is

$$
G^{17}OP_C = K\,(O_2)_{eq}\frac{\left(\frac{X^{17}-X_{eq}^{17}}{X^{17}}\right) - \lambda\left(\frac{X^{18}-X_{eq}^{18}}{X^{18}}\right)}{\left(\frac{X_p^{17}-X^{17}}{X^{17}}\right) - \lambda\left(\frac{X_p^{18}-X^{18}}{X^{18}}\right)} \\
+ D\,(O_2)_{thr}\frac{\left(\frac{X^{17}-X_{thr}^{17}}{X^{17}}\right) - \lambda\left(\frac{X^{18}-X_{thr}^{18}}{X^{18}}\right)}{\left(\frac{X_p^{17}-X^{17}}{X^{17}}\right) - \lambda\left(\frac{X_p^{18}-X^{18}}{X^{18}}\right)},
\tag{4}
$$

where $G^{17}OP_C$ is the $G^{17}OP$ corrected for turbulent flux of O_2 from the thermocline. For convenience we will abbreviate the GOP correction for turbulent flux of O_2 from the thermocline (the second term on the right-hand side in Eq. 4) to "TFC" hereafter. The numerator of the TFC represents the contribution of the turbulent flux to the GOP estimated from $^{17}\Delta$ in the ML.

3 Simulations by a 1-D numerical model

We used a simple 1-D model, which simulated the effects of GOP, respiration, gas exchange and turbulence on each O_2 isotopologue, to compare the $G^{17}OP$ rates obtained by Eq. (4) with those obtained without applying the TFC. Briefly, the model simulated the water column up to a depth of 300 m, which was divided into 30 layers of 10 m each, and calculated the fluxes of each O_2 isotopologue in each layer produced by photosynthesis, respiration, and turbulent
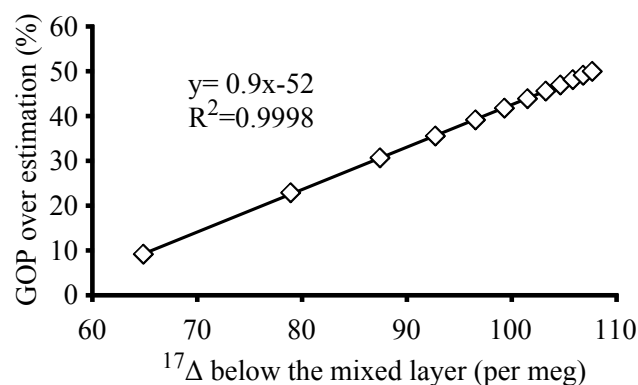
Fig. 2. Linear regression analysis of model simulation results, showing the increase in mixed-layer GOP overestimation $((G^{17}OP_{PRO}/GOP_M - 1)\cdot 100)$ versus $^{17}\Delta$ below the mixed layer.

mixing (model equations, parameters and MATLAB files are given in the Supplement). An additional layer at the top of the water column represented the ocean surface. In this layer, (O_2) and its isotopic composition were kept in air–sea equilibrium. The eddy-diffusivity coefficient in the ML $(2.5 \times 10^{-3}\,\mathrm{m^2\,s^{-1}})$ was assigned so as to let (O_2) in the ML be fully mixed. The concentration of each isotopologue in the ML was affected by turbulent mixing with the uppermost layer, photosynthesis, respiration and turbulent mixing with the seasonal thermocline residing below. For the seasonal thermocline, we used $\kappa = 10^{-4}\,\mathrm{m^2\,s^{-1}}$ (see sensitivity tests section).

We ran two simulations to examine the effect of turbulent mixing on ML $G^{17}OP$. In the "fixed mixing depth" simulation (Table 1) we ran the model with a constant ML depth of 40 m. The layer directly below the ML base, at 50 m, was assigned as the "thermocline" data point for TFC calculation. ML $\delta^{17}O$, $\delta^{18}O$ and $^{17}\Delta$ values were calculated every 30 model time steps (model month). In the first model month of the simulation, $G^{17}OP_{LB}$ and $G^{17}OP_{PRO}$ slightly overestimated (by 7 %) the GOP assigned in the model (GOP_M). In the following model months, the overestimation of both $G^{17}OP_{LB}$ and $G^{17}OP_{PRO}$ increased, reaching ~ 40 % after 5 model months. As shown in Fig. 2, the increase in GOP overestimation was closely related to the increase in $^{17}\Delta$ in the seasonal thermocline. However, $G^{17}OP_C$, which corrects for the turbulent mixing flux of O_2 from the thermocline, remained constant with a slight underestimation of ~ 7 % throughout the entire simulation period. When we effectively shut down turbulent mixing in the model by reducing κ within the thermocline to $10^{-6}\,\mathrm{m^2\,s^{-1}}$, $G^{17}OP_{LB}$ and $G^{17}OP_{PRO}$ were in good agreement with GOP_M. This indicates that turbulent flux was indeed the cause of the overestimation.

In the "varying mixing depth" simulation, ML depths were allowed to change, roughly according to the typical monthly variations in BATS station (Table 2). When

Table 1. Results of model simulation with a constant mixed-layer depth of 40 m GOP-M – input GOP rate, $G^{17}OP_{LB}$ – Luz and Barkan (2000), $G^{17}OP_{PRO}$ – Prokopenko et al. (2011), $G^{17}OP_C$ – this work includes a correction for turbulent flux of O_2 from the thermocline. All GOP rates are in mmol m^{-2} day^{-1}. In the columns marked with t, $\kappa = 10^{-4}$ m^2 s^{-1}, whereas in the columns marked with nt, $\kappa = 10^{-6}$ m^2 s^{-1}, which effectively shuts down the turbulent flux of O_2 between the thermocline and the mixed layer.

Time step (day)	GOP-M^t	$G^{17}OP^t_{LB}$	$G^{17}OP^t_{PRO}$	$G^{17}OP^t_C$	$G^{17}OP^{nt}_{LB}$	$G^{17}OP^{nt}_{PRO}$
30		112	117	98	100	104
60		126	132	101	102	106
90		134	140	101	102	107
120		139	146	101	102	107
150		143	149	101	103	107
180	107	146	152	100	103	108
210		148	155	100	103	108
240		150	156	100	103	108
270		151	158	100	104	108
300		152	159	100	104	109
330		153	160	100	104	109
360		154	161	99	104	109

ML depth underwent rapid changes (in the model months corresponding to January–March and August–December in BATS), the steady-state assumption was not valid, and neither $G^{17}OP_{LB}$ and $G^{17}OP_{PRO}$, nor $G^{17}OP_C$ yielded GOP rates comparable to GOP$_M$. On the other hand, when the ML depth experienced small variations (in the months when ML depth corresponded to April–August in BATS), $G^{17}OP_C$ rates were close to GOP$_M$, while $G^{17}OP_{LB}$ and $G^{17}OP_{PRO}$ were about 60–90 % greater than GOP$_M$.

4 Sensitivity tests

In addition to simulating the effect of turbulent mixing on GOP estimations, we used the 1-D model to test the sensitivity of the TFC to the depth of the "thermocline" reference point, to the analytical error associated with $^{17}\Delta$ measurements, and to the ML depth.
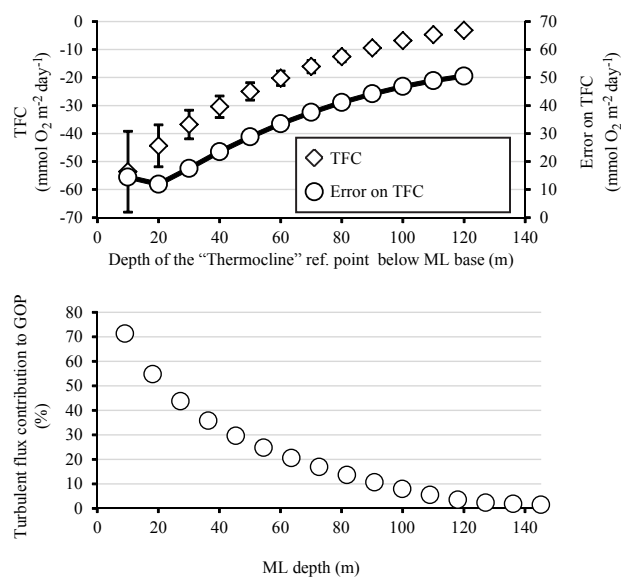
The choice of the depth which represents the "thermocline" point can affect the resulting GOP (Fig. 1). While the TFC assumes a linear $^{17}\Delta$ gradient between the ML and the "thermocline", the actual $^{17}\Delta$ gradient is not necessarily so. Therefore, the closer the "thermocline" point to the ML base, the better it represents the actual fluxes of O_2 isotopolouges between the ML and the thermocline (Fig. 1). On the other hand, the difference in the isotopic composition between the ML and the "thermocline" has to be considerably larger than the analytical error associated with $^{17}\Delta$ measurements (~ 7 per meg; e.g. Reuer et al., 2007). In order to assess the sensitivity of the TFC to the depth of the "thermocline" reference point and to the analytical error on $^{17}\Delta$, we calculated the magnitude of the turbulence correction with different "thermocline" reference points. As illustrated in Fig. 3a, the magnitude of the TFC decreased as the distance between the ML

base and the "thermocline" reference point increased. Assuming that the TFC calculated using the "thermocline" immediately (10 m) below the ML is the most accurate, we consider the difference between this value and the TFC calculated for other "thermocline" depths as the error induced on the TFC by the selection of the "thermocline" depth. Using the same 1-D model simulations, we calculated the effect of the analytical error associated with $^{17}\Delta$ measurements on the magnitude of the TFC. For this end, we calculated the TFC three times per each "thermocline" depth. The first TFC was calculated without error on $^{17}\Delta$ values, whereas for the other two, a 7 per meg error was either added or subtracted from the $^{17}\Delta$ values of the ML and the "thermocline". The combinations which yielded the maximal deviations from the no-error TFC are illustrated by the vertical error bars in Fig. 3a. The magnitude of this error decreased with increasing depth of the "thermocline". Finally, we estimated the combined effect of the choice of the "thermocline" depth and the analytical error on the TFC, by propagating these two errors. The resulting error is illustrated in Fig. 3a. For the scenario used in our tests, the minimal error (~ 20 %) was observed at 20 m below the ML base. We note that this error is likely to be an overestimation of the actual error which results from these two factors, since we used the maximal analytical error on both ML $^{17}\Delta$ and $^{17}\Delta_{thr}$ values simultaneously, and in reverse directions, which yielded the maximal effect on the resulting $^{17}\Delta$ gradient. Moreover, as the ML $^{17}\Delta$ value is usually an average of several measurements, it is likely to be subject to a much smaller error than 7 per meg.

The magnitude of the TFC is linearly dependent on the value of κ used in Eq. (4). However, our simulations also showed that using κ values smaller than 1×10^{-4} m^2 s^{-1}, yielded $^{17}\Delta$ values in the thermocline that were higher than 200 per meg, and when we used $\kappa = 0.5 \times 10^{-4}$ m^2 s^{-1} $^{17}\Delta$

Table 2. Results of model simulation of GOP with varying mixed-layer depth ML – mixed layer, GOP-M – input GOP rate, G^{17}OP$_{LB}$ – Luz and Barkan (2000), G^{17}OP$_{PRO}$ – Prokopenko et al. (2011), G^{17}OP$_C$ – this work includes a correction for turbulent flux of O$_2$ from the thermocline. All GOP rates are in mmol m^{-2} day^{-1}. In the columns marked with t, $\kappa = 10^{-4}$ m^2 s^{-1}, whereas in the columns marked with nt, $\kappa = 10^{-6}$ m^2 s^{-1}, which effectively shuts down the turbulent flux of O$_2$ between the thermocline and the mixed layer.

Time step (day)	ML depth (m)	GOP-M^t	G^{17}OP$^t_{LB}$	G^{17}OP$^t_{PRO}$	G^{17}OP^t_C	G^{17}OP$^{nt}_{LB}$	G^{17}OP$^{nt}_{PRO}$
30	200	226	111	115	132	112	116
60	250	226	136	142	162	137	142
90	10	30	87	91	82	84	88
120	20	58	91	95	54	58	61
150	20	58	97	102	51	55	58
180	20	58	103	108	51	56	58
210	20	58	107	112	50	56	59
240	40	107	204	212	129	228	237
270	80	180	332	341	258	410	418
300	90	193	264	273	224	262	271
330	100	204	249	257	220	253	262
360	140	226	273	281	262	305	313

Fig. 3. Sensitivity of the turbulent-flux correction. **(a)** The sensitivity of the GOP correction for turbulent flux of O$_2$ from the thermocline (TFC) to the depth of the "thermocline" reference point below the mixed layer (ML). The error bars represent the maximal error on the TFC, induced by the analytical error associated with $^{17}\Delta$ measurements (7 per meg). The error resulting from the combination of these two factors (circles) on the TFC shows a minimum at 20 m below ML. **(b)** The relative contribution of turbulent mixing flux to estimated G17OP as a function of the ML depth. Model conditions for each sensitivity test are described in Sect. 4 in the text.

values in the thermocline approached maximal values (~ 250 per meg), whereas observed summer values in the thermocline do not exceed 160 per meg (Juranek and Quay, 2005, Quay et al., 2010) in the Hawaii Ocean time-series (HOT) station and similar values in Bermuda Atlantic time-series

(BATS) station (Nicholoson et al., 2011). Moreover, Nicholson et al. (2012) used similar values (8–9×10^{-5} m^2 s^{-1}) to reproduce the physical conditions (ML depth, heat content and sea surface temperature) in the upper 1000 m in the BATS and in HOT. Therefore, we estimate that our choice of κ was rather accurate for the processes of turbulent mixing between the ML and the seasonal thermocline. Apparently, in spite of the fact that 1×10^{-4} m^2 s^{-1} is almost an order of magnitude higher than the value estimated from SF$_6$ release experiments in the permanent thermocline (~ 300 m, Ledwell et al., 1993), κ values near the interface between the ML and the thermocline are higher than those which characterize the thermocline at greater depths where SF$_6$ release experiments were conducted. Given the highly unrealistic profiles we obtained for lower values and the agreement between our model and the model used by Nicholson et al. (2012), we assume an uncertainty of ~ 50 % on this value, and consequently, a 50 % uncertainty on the TFC term.

Finally, we tested the sensitivity of the TFC to the ML depth. The results (Fig. 3b) show that as the ML depth increases, the contribution of turbulence to the uncorrected GOP decreases. This implies that correcting G^{17}OP rates for turbulent fluxes of O$_2$ isotopologues from the thermocline is especially important in ocean areas in which the summer ML is relatively shallow, such as in BATS.

5 The effect of turbulent mixing on measured GOP rates

To estimate the effect of turbulent mixing on G^{17}OP estimations in the ocean, we compared previously published GOP rates from BATS (Luz and Barkan, 2009) with equivalent G^{17}OP$_C$ rates. In addition, we used published data (Nicholson et al., 2012) to calculate and compare between G^{17}OP$_{LB}$

and G^{17}OP$_C$ in Hawaii Ocean time series (HOT). To use the TFC, we chose months in which vertical profiles of $^{17}\Delta$ and O$_2$ were measured and published (Nicholson et al., 2012). Following our conclusions from the 1-D model simulations, we compared months in which there were no major changes in ML depth. The κ values for BATS and HOT were both taken from Nicholson et al. (2012).

ML depth was determined as the depth in which a difference of 0.5 % in O$_2$ concentration relative to the sea surface was observed (Castro-Morales and Kaiser, 2012). The "thermocline" reference point was assigned as the depth nearest to the ML base in which $^{17}\Delta$ was at least 14 per meg larger than $^{17}\Delta$ in the ML. In BATS, K values were obtained from Luz and Barkan (2009). In HOT, wind speed data from $\sim$ 10 days before the cruise were obtained from QuickScat database, and K was estimated according to Sweeney et al. (2007). The results (Table 3) showed that G^{17}OP$_C$ rates were 65–100 % lower than G^{17}OP$_{LB}$ in BATS, and 10–40 % lower in HOT. These results are in agreement with Nicholson et al. (2012), who estimated the effect of mixing as 60–90 % of G^{17}OP. We note that Luz and Barkan (2009) used Wanninkhof (1992) parameterization for K in BATS. Applying more recent parameterization (Ho et al., 2006; Sweeny et al., 2007), which gives lower estimates of gas-exchange rates, would result in an even greater contribution of the O$_2$ turbulent flux from the thermocline.

6 Discussion

Our results showed that vertical turbulence of O$_2$ from the thermocline, affects ML G^{17}OP estimations, such that corrected G^{17}OP rates are considerably lower than the uncorrected rates. This indicates that a large fraction of the ML photosynthetic O$_2$ is not produced in the ML itself, but rather in the thermocline below it. However, our results also show that the turbulent contribution to the ML $^{17}\Delta$ can be corrected in a rather simple manner. While the correction itself was derived using several approximations, such as constant ML depth, and constant $^{17}\Delta$ gradient between the thermocline and the ML, most of the resulting uncertainties also exist in the uncorrected equations for G^{17}OP (Luz and Barkan 2000, Prokopenko et al., 2010). These uncertainties are intrinsic to any extrapolation in time and space of GOP rates estimations from a "snap-shot" profile. Moreover, our sensitivity tests showed that the uncertainty on the TFC is smaller than 50 %, and therefore, we concluded that in spite of the approximations and uncertainties involved, using the TFC will improve the accuracy of G^{17}OP estimations. Below, we discuss the technical aspects and the implications of these findings.

6.1 Applying GOP correction for turbulent flux of O$_2$ from the thermocline in oceanographic measurements

Our results showed that when the ML depth does not change considerably, the effect of turbulent flux on ML GOP estimation can be corrected. However, to apply the correction, at least one point of data, which includes [O$_2$] and its isotopic composition below the ML is necessary. Such data points are easy to obtain in time-series study sites, such as BATS and HOT, but can complicate basin-wide G^{17}OP estimations, which usually rely on underway seawater systems installed on ships of opportunity for sampling (Juranek and Quay, 2010; Juranek et al., 2012). In the future, such studies would need to either collect several representative "thermocline" samples from the thermocline along the cruise route, or use existing data if available to apply the TFC. Such corrections could also be applied to existing data.

The TFC is sensitive to the exact depth of the "thermocline" data point (Fig. 3a), and to the analytical error on $^{17}\Delta$ measurements. Technical improvements which would reduce the error on $^{17}\Delta$ measurements would also increase the accuracy of G^{17}OP estimations in general, and the accuracy of the TFC in particular. As shown in Fig. 3a, the error induced on the TFC by the analytical error, decreases with the depth selected for the "thermocline", while the error induced by deviation of the $^{17}\Delta$ profile from a linear one increases with depth. In the depth range immediately below the ML base, these effects cancel each other to some extent, and an optimal depth can be estimated. This depth is dependent on the vertical distribution of $^{17}\Delta$ in each study-site, and on the analytical error associated with the $^{17}\Delta$ measurement process applied. In practical terms, we suggest using the minimum depth in which the $^{17}\Delta$ value is significantly (within the analytical uncertainty) different than the ML value.

Previous knowledge of $^{17}\Delta$ dynamics for the study site would help with choosing the optimal depth to collect the "thermocline" sample. For example, Juranek and Quay (2005) and Quay et al. (2010) have shown that during summer months in HOT, differences greater than 60 per meg (an order of magnitude higher than the analytical error) between the ML and thermocline $^{17}\Delta$ could be found within 20–40 m below the ML base. In BATS, $^{17}\Delta$ gradients tend to be smaller, and a difference of 60 per meg can usually be found 40–60 m below the ML depth (Nicholson et al., 2012). Therefore, the "thermocline" optimal depth is likely to be shallower in HOT than in BATS, and consequently, associated with a smaller error.

6.2 Parameterization of gas exchange and eddy diffusivity

The TFC, and consequently G^{17}OP$_C$ are sensitive to the accuracy of both K and κ. While the sensitivity to K characterizes G^{17}OP in general, a combination of errors on K and

Table 3. Comparison of $G^{17}OP$ rates from BATS and HOT ML – mixed layer, $G^{17}OP_{LB}$ – Luz and Barkan (2000), "thermocline" – depth of the data point representing the thermocline. $G^{17}OP_C$ – $G^{17}OP$ corrected for turbulent flux of O_2 from the thermocline. All the parameters used for the calculations made in BATS were taken from Luz and Barkan (2009). κ values and the raw data used for the calculation of $G^{17}OP_{LB}$ and $G^{17}OP_C$, and the parameters used for the calculations in HOT were taken from Nicholson et al. (2012). ML depth was determined as the depth in which a difference of 0.5 % in O_2 concentration relative to the sea surface was observed. Gas-exchange rates in HOT were calculated according to Sweeney et al. (2007) from wind speed data obtained from QuickSCAT.

Location	Date	κ $(\mathrm{m^2\,s^{-1}})$	ML (m) depth	"thermocline" (m) depth	$G^{17}OP_{LB}$	$G^{17}OP_C$ (mmol m^{-2} day^{-1})
BATS	May, 2000		20	40	29	9
	July, 2000	9×10^{-5}	20	80	45	16
	September, 2000		20	40	50	−4
HOT	May, 2007	8×10^{-5}	100	125	131	116
	August, 2007		45	100	37	20

κ may yield inaccurate $G^{17}OP_C$ rates. We assume that the negative $G^{17}OP_C$ rate that we obtained in BATS in September 2000 (Table 3) was the result of inaccurate choice of K and κ. We also acknowledge the fact that the uncertainty on κ is the largest source of error on the magnitude of the TFC. Since the main aims of this work were to show the importance of turbulence effects and to suggest a correction, rather than to perform accurate GOP estimations, we used crude estimations of K and κ. However, the fact that $^{17}\Delta$ in the ML depends upon GOP, gas-exchange and turbulent flux from the thermocline, means that in future studies any one of these three parameters could be estimated by performing simultaneous measurements of the other two parameters. For example, if GOP is estimated by ^{18}O incubations and gas exchange is estimated from wind speed measurements, $^{17}\Delta$ profiles could be used to estimate κ in the seasonal thermocline. Moreover, since ^{18}O incubations are not affected by turbulence, it is likely that provided that K and κ are accurately parameterized, $G^{17}OP_C : N^{14}CP$ would agree with $G^{18}OP : N^{14}CP$ (Marra, 2002).

7 Conclusions

1. Turbulent fluxes of O_2 isotopologues from the thermocline have a pronounced effect over $^{17}\Delta$ values in the ML, and consequently, over the accuracy of $G^{17}OP$ estimations.

2. An accurate $G^{17}OP$ estimate can be obtained by using a simple correction for the effect of the turbulent fluxes.

3. The main source of uncertainty on the GOP correction for turbulent flux of O_2 from the thermocline is the eddy-diffusivity coefficient, which causes ~ 50 % uncertainty.

4. The GOP correction for turbulent flux of O_2 from the thermocline is applicable when the mixed-layer depth

does not change sharply, and requires measurements of O_2 and its isotopic composition in a single point below the mixed layer, in addition to the standard measurements of these values in the mixed layer.

Appendix A

Derivation of the term for correcting mixed-layer gross O_2 production to turbulent flux of O_2 from the thermocline

Like Prokopenko et al. (2011), we consider a surface mixed-layer subject to respiration, photosynthesis and gas exchange with the atmosphere, but which also exchanges water with the underlying "thermocline" layer via turbulent diffusion. In the current box model framework, we parameterize the turbulent O_2 flux with the "thermocline" layer as

$$-\frac{\kappa}{Z}\left((O_2) - (O_2)_{\mathrm{thr}}\right), \tag{A1}$$

where (O_2) and $(O_2)_{\mathrm{thr}}$ are the dissolved O_2 concentrations in the mixed layer and in the thermocline, respectively. κ is the eddy diffusion coefficient and Z is the vertical distance between the base of the ML and the depth assigned as "thermocline". For convenience, we use $D = \kappa/Z$ hereafter. Likewise, turbulent fluxes of O_2 isotopes are parameterized as

$$-D\left((O_2)X^* - (O_2)_{\mathrm{thr}}X^*_{\mathrm{thr}}\right), \tag{A2}$$

where X^* represents the ratio $^*O/^{16}O$. The mass balances for O_2 and its isotopes are given by

$$h\frac{\partial((O_2))}{\partial t} = \mathrm{GOP} - R - K\left((O_2) - (O_2)_{\mathrm{eq}}\right) \\ - D\left((O_2) - (O_2)_{\mathrm{thr}},\right) \tag{A3}$$

$$h\frac{\partial((O_2)X^*)}{\partial t} = \mathrm{GOP}X^*_p - R\alpha^*X^* - K \\ \left((O_2)X^* - (O_2)_{\mathrm{eq}}X^*_{\mathrm{eq}}\right) - D\left((O_2)X^* - (O_2)_{\mathrm{thr}}X^*_{\mathrm{thr}}\right) \tag{A4}$$

where h is the mixed-layer depth, t is time, GOP is the gross O$_2$ production, R is the respiration rate and K is the piston velocity. α^* is the fractionation factor associated with respiration for each isotopologue. The subscripts "p" and "eq" denote "photosynthetic" and "equilibrium", respectively.

The remainder of the derivation is carried out by straightforward applications of the steps outlined in Prokopenko et al. (2011), and repeated here for the sake of completion. The left-hand side of Eq. (A4) can be written explicitly as

$$h \frac{\partial((O_2)X^*)}{\partial t} = hX^* \frac{\partial((O_2))}{\partial t} + h(O_2) \frac{\partial(X^*)}{\partial t}. \tag{A5}$$

Upon substituting the left-hand side, and the first term on the right-hand side of Eq. (A3) with Eq. (A4) and Eq. (A3), respectively, rearranging and dividing by X* one gets

$$\begin{aligned} h(O_2) \frac{1}{X^*} \frac{\partial(X^*)}{\partial t} &= GOP \left(\frac{X_p^* - X^*}{X^*} \right) + R(1 - \alpha^*) \\ &+ K(O_2)_{eq} \left(\frac{X_{eq}^* - X^*}{X^*} \right) + + D(O_2)_{thr} \left(\frac{X_{thr}^* - X^*}{X^*} \right). \end{aligned} \tag{A6}$$

Note that the left-hand side of Eq. (A6) is equal to $h(O_2) \frac{\partial(\ln X^*)}{\partial t}$. On the other hand, ^{17}O excess is defined as

$$^{17}\Delta = \ln(\delta^{17}O + 1) - \lambda \ln(\delta^{18}O + 1). \tag{A7}$$

Taking the derivative of Eq. (A7) with respect to time and multiplying by $h(O_2)$ yields

$$h(O_2) \frac{\partial(^{17}\Delta)}{\partial t} = h(O_2) \left(\frac{\partial(\ln X^{17})}{\partial t} - \lambda \frac{\partial(\ln X^{18})}{\partial t} \right). \tag{A8}$$

Substituting Eq. (A6) into Eq. (A8) yields

$$\begin{aligned} h(O_2) \frac{\partial(^{17}\Delta)}{\partial t} = G^{17}OP_C &\left[\left(\frac{X_p^{17} - X^{17}}{X^{17}} \right) - \lambda \left(\frac{X_p^{18} - X^{18}}{X^{18}} \right) \right] \\ &- K(O_2)_{eq} \left[\left(\frac{X^{17} - X_{eq}^{17}}{X^{17}} \right) - \lambda \left(\frac{X^{18} - X_{eq}^{18}}{X^{18}} \right) \right] \\ &- D(O_2)_{thr} \left[\left(\frac{X^{17} - X_{thr}^{17}}{X^{17}} \right) - \lambda \left(\frac{X^{18} - X_{thr}^{18}}{X^{18}} \right) \right], \end{aligned} \tag{A9}$$

where G^{17}OP$_C$ is the turbulence-corrected G^{17}OP. Note, the respiration term is not affected by the addition of the turbulent-flux term and is cancelled out in the expression for the changes in ^{17}O excess, as expected.

Finally, for a mixed layer in steady state, we obtain the following expression for GOP corrected for turbulent diffusion:

$$\begin{aligned} G^{17}OP_C = \ &K(O_2)_{eq} \frac{\left(\frac{X^{17} - X_{eq}^{17}}{X^{17}} \right) - \lambda \left(\frac{X^{18} - X_{eq}^{18}}{X^{18}} \right)}{\left(\frac{X_p^{17} - X^{17}}{X^{17}} \right) - \lambda \left(\frac{X_p^{18} - X^{18}}{X^{18}} \right)} \\ &+ D(O_2)_{thr} \frac{\left(\frac{X^{17} - X_{thr}^{17}}{X^{17}} \right) - \lambda \left(\frac{X^{18} - X_{thr}^{18}}{X^{18}} \right)}{\left(\frac{X_p^{17} - X^{17}}{X^{17}} \right) - \lambda \left(\frac{X_p^{18} - X^{18}}{X^{18}} \right)}. \end{aligned} \tag{A10}$$

References

Castro-Morales, K., Cassar, N., Shoosmith, D. R., and Kaiser, J.: Biological production in the Bellingshausen Sea from oxygen-to-argon ratios and oxygen triple isotopes, Biogeosciences, 10, 2273–2291, doi:10.5194/bg-10-2273-2013, 2012a.

Castro-Morales, K. and Kaiser, J.: Using dissolved oxygen concentrations to determine mixed layer depths in the Bellingshausen Sea, Ocean Sci., 8, 1–10, doi:10.5194/os-8-1-2012, 2012b.

Ho, D. T., Law, C. S., Smith, M. J., Schlosser, P., Harvey, M., and Hill, P.: Measurements of air-sea gas exchange at high wind speeds in the Southern Ocean: Implications for global parameterizations, Geophys. Res. Lett., 33, L16611, doi:10.1029/2006GL026817, 2006.

Jonsson, B. F., Doney, S. C., Dunne, J., and Bender, M.: Evaluation of Southern Ocean O$_2$/Ar based NCP estimates in a model framework, J. Geophys. Res.-Biogeo., 118, 385–399, doi:10.1002/jgrg.20032, 2013.

Juranek, L. W. and Quay, P. D.: In vitro and in situ gross primary and net community production in the North Pacific Subtropical Gyre using labeled and natural abundance isotopes of dissolved O$_2$, Global Biogeochem. Cy., 19, Gb3009, doi:10.1029/2004gb002384, 2005.

Juranek, L. W. and Quay, P. D.: Basin-wide photosynthetic production rates in the subtropical and tropical Pacific Ocean determined from dissolved oxygen isotope ratio measurements, Global Biogeochem. Cy., 24, Gb2006, doi:10.1029/2009gb003492, 2010.

Juranek, L. W., Quay, P. D., Feely, R. A., Lockwood, D., Karl, D. M., and Church, M. J.: Biological production in the NE Pacific and its influence on air-sea CO$_2$ flux: Evidence from dissolved oxygen isotopes and O$_2$/Ar, J. Geophys. Res.-Oceans, 117, C05022, doi:10.1029/2011jc007450, 2012.

Juranek, L. W. and Quay, P. D.: Using triple isotopes of dissolved oxygen to evaluate global marine productivity, Ann. Rev. Mar. Sci., 5, 503–524, doi:10.1146/annurev-marine-121211-172430, 2013.

Kaiser, J.: Technical note: Consistent calculation of aquatic gross production from oxygen triple isotope measurements, Biogeosciences, 8, 1793–1811, doi:10.5194/bg-8-1793-2011, 2011.

Kaiser, J. and Abe, O.: Reply to Nicholson's comment on "Consistent calculation of aquatic gross production from oxygen triple isotope measurements" by Kaiser (2011), Biogeosciences, 9, 2921–2933, doi:10.5194/bg-9-2921-2012, 2012.

Ledwell, J. R., Watson, A. J., and Law, C. S.: Evidence for slow mixing across the pycnocline from an open-ocean tracer-release, Nature, 364, 701–703, doi:10.1038/364701a0, 1993.

Luz, B., Barkan, E., Bender, M. L., Thiemens, M. H., and Boering, K. A.: Triple-isotope composition of atmospheric oxygen as a tracer of biosphere productivity, Nature, 400, 547–550, doi:10.1038/22987, 1999.

Luz, B. and Barkan, E.: Assessment of oceanic productivity with the triple-isotope composition of dissolved oxygen, Science, 288, 2028–2031, doi:10.1126/science.288.5473.2028, 2000.

Luz, B. and Barkan, E.: The isotopic ratios $^{17}O/^{16}O$ and $^{18}O/^{16}O$ in molecular oxygen and their significance in biogeochemistry, Geochim. Cosmochim. Ac., 69, 1099–1110, doi:10.1016/j.gca.2004.09.001, 2005.

Luz, B. and Barkan, E.: Net and gross oxygen production from O_2/Ar, $^{17}O/^{16}O$ and $^{18}O/^{16}O$ ratios, Aqut. Microb. Ecology, 56, 133–145, doi:10.3354/ame01296, 2009.

Luz, B. and Barkan, E.: Oxygen isotope fractionation in the ocean surface and $^{17}O/^{16}O$ of atmospheric O_2, Global Biogeochem. Cy., 25, Gb4006, doi:10.1029/2011gb004178, 2011a.

Luz, B. and Barkan, E.: Proper estimation of marine gross O_2 production with $^{17}O/^{16}O$ and $^{18}O/^{16}O$ ratios of dissolved O_2, Geophys. Res. Lett., 38, L19606, doi:10.1029/2011gl049138, 2011b.

Marra, J.: Approaches to the measurement of plankton production, in: Phytoplankton productivity: carbon assimilation in marine and freshwater ecosystems, edited by: Williams, P. J., Thomas, D. N., and Reynolds, R. C., Blackwell Science, Malden, MA, 78–108, 2002.

Miller, M. F.: Isotopic fractionation and the quantification of ^{17}O anomalies in the oxygen three-isotope system: an appraisal and geochemical significance, Geochim. Cosmochim. Ac., 66, 1881–1889, doi:10.1016/s0016-7037(02)00832-3, 2002.

Nicholson, D. P.: Comment on: "Technical note: Consistent calculation of aquatic gross production from oxygen triple isotope measurements" by Kaiser (2011), Biogeosciences, 8, 2993–2997, doi:10.5194/bg-8-2993-2011, 2011.

Nicholson, D. P., Stanley, R. H. R., Barkan, E., Karl, D. M., Luz, B., Quay, P. D., and Doney, S. C.: Evaluating triple oxygen isotope estimates of gross primary production at the Hawaii Ocean Time-series and Bermuda Atlantic Time-series Study sites, J. Geophys. Res-Oceans, 117, C05012, doi:10.1029/2010jc006856, 2012.

Prokopenko, M. G., Pauluis, O. M., Granger, J., and Yeung, L. Y.: Exact evaluation of gross photosynthetic production from the oxygen triple-isotope composition of O_2: Implications for the net-to-gross primary production ratios, Geophys. Res. Lett., 38, L14603, doi:10.1029/2011gl047652, 2011.

Quay, P. D., Peacock, C., Bjoerkman, K., and Karl, D. M.: Measuring primary production rates in the ocean: Enigmatic results between incubation and non-incubation methods at Station ALOHA, Global Biogeochem. Cy., 24, Gb3014, doi:10.1029/2009gb003665, 2010.

Reuer, M. K., Barnett, B. A., Bender, M. L., Falkowski, P. G., and Hendricks, M. B.: New estimates of Southern Ocean biological production rates from O_2/Ar ratios and the triple isotope composition of O_2, Deep-Sea Res. Pt.I, 54, 951–974, doi:10.1016/j.dsr.2007.02.007, 2007.

Sarma, V. V. S. S., Abe, O., Hinuma, A., and Saino, T.: Short-term variation of triple oxygen isotopes and gross oxygen production in the Sagami Bay, central Japan, Limnol. Oceanogr., 51, 1432–1442, doi:10.4319/lo.2006.51.3.1432, 2006.

Sweeney, C., Gloor, E., Jacobson, A. R., Key, R. M., McKinley, G., Sarmiento, J. L., and Wanninkhof, R.: Constraining global air-sea gas exchange for CO_2 with recent bomb ^{14}C measurements, Global Biogeochem. Cy., 21, GB2015, doi:10.1029/2006GB002784/abstract, 2007.

Wanninkhof, R.: Relationship between wind-speed and gas-exchange over the ocean, J. Geophys. Res-Oceans, 97, 7373–7382, doi:10.1029/92jc00188, 1992.